Geoderma 441 (2024) 116734

Contents lists available at ScienceDirect

Geoderma

journal homepage: www.elsevier.com/locate/geoderma

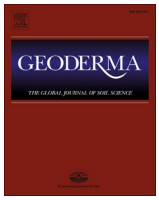

Accelerated weathering of silicate rock dusts predicts the slow-release liming in soils depending on rock mineralogy, soil acidity, and test methodology

Robrecht Van Der Bauwhede [a,*], Bart Muys [a], Karen Vancampenhout [b], Erik Smolders [c]

[a] Division Forest, Nature and Landscape, KU Leuven, 3001 Leuven, Celestijnenlaan 200E, Box 2411, Belgium
[b] Division Forest, Nature and Landscape, KU Leuven Campus Geel, Kleinhoefstraat 4, 2240 Geel, Belgium
[c] Division of Soil and Water Management, KU Leuven, 3001 Leuven, Kasteelpark Arenberg 20, Belgium

ARTICLE INFO

Handling Editor: A. Margenot

Keywords:
Silicate rock powder
Acid soil restoration
Soil suspension test
Outdoor soil mesocosm
Dissolution rates
Soil pH
Enhanced rock weathering (ERW)
Weathering rates
Acid Neutralising Capacity (ANC)

ABSTRACT

The ongoing acidification of soil poses a significant threat to the proper functioning of various ecosystems worldwide. Silicate rock dusts (RD) are increasingly amended to acid soils to restore their pH, but the acid neutralising capacity (ANC) and dissolution rate of these products are highly variable and lack proper assessment protocols. It is expected that pH-dependent RD ANCs and dissolution rates dictate the pH increase in soils depending on the initial pH and pH buffer power of the soil. This study addressed these questions by comparing and validating three accelerated weathering tests for their capacity to predict the gradual liming effects in a two-year outdoor mesocosm. Five commercial RDs (two basalts, phonolite, foidite, and trachy-andesite) were tested in four acidified forest soils varying in initial pH, in texture and associated pH buffer power. First, RD dissolution was measured in aqueous batch renewal systems during one year at various starting pH (3.5, 4.5, and 5.5) and constant temperatures (20 °C, 37 °C, and 65 °C). These showed that the ANCs of RDs exhibit a fast fraction (half-life < 1 day) followed by a slower fraction. Second, titration tests of RDs at fixed solution pH, i.e., pH_{stat}, performed between pH 3.5 and 4.5 revealed surface normalised dissolution rates that decreased factors 10–100 per unit pH increase, the slope depending on the RD's mineralogy. Indeed, the rate ranking of observed surface area normalised dissolution rates confirmed that of literature-based values, weighed by the XRD-derived mineralogical fractions. Third, lime-calibrated agitated soil-RD suspension tests were conducted for two months, illustrating the dependency of RD ANC on soil context, and yielding ANCs that were factor 2–5 times larger than in the batch renewal test because of pH buffering effects of soil particulates. Finally, an outdoor soil mesocosm on the four acid soils amended with RDs at 12 Mg/ha and 340 Mg/ha was established and soil pH was monitored for 2 years. The observed pH trends corresponded well for both the low dose ($R^2_a = 0.67$) and the high dose ($R^2_a = 0.93$) with model predictions made using the pH- and temperature-dependent RD dissolution rates (pH_{stat} test) and the soil pH buffer power and RD slow ANC-fraction (soil-RD suspension test). This model predicts half-lives of RD dissolution ranging between <1 month to >100 years depending on the starting pH of the soil, its pH buffer power, the RD mineralogy (XRD based) and its specific surface area. This study shows that the dissolution and ANC of RD can be most pragmatically predicted with a series of lime-calibrated soil-RD suspension tests of maximally two months.

1. Introduction

Soil acidification is threatening the functioning of (agro)ecosystems on 30–40 % of the land surface of our planet (Ulrich and Sumner, 2012). Low soil pH adversely affects nutrient cycling both in intensely weathered soils in the southern Hemisphere as in soils impacted by acidifying atmospheric depositions in the northern Hemisphere, and more restoration efforts should be implemented as urgently stressed in the United Nations Decade on Ecosystem Restoration (FAO et al., 2023; Schulte-Uebbing et al., 2022; Slessarev et al., 2016). Furthermore, the ongoing disruption of the nitrogen cycle is leading to net acidification and eutrophication in soils, thereby creating nutrient imbalances which

* Corresponding author.
E-mail address: robrecht.vanderbauwhede@kuleuven.be (R. Van Der Bauwhede).

https://doi.org/10.1016/j.geoderma.2023.116734
Received 12 May 2023; Received in revised form 28 November 2023; Accepted 29 November 2023
Available online 8 December 2023

above the critical deposition loads lead to distinct adverse effects in species' functioning and composition (Bobbink et al., 2023; Nilsson, 1988; Schulze et al., 1989; Vogels et al., 2023). The conventional approach to increase soil pH and buffering of acid soils is liming e.g. CaO, $Ca(OH)_2$, or $Ca_xMg_{1-x}CO_3$ (Oates, 2008). These products have a large acid neutralising capacity (ANC), i.e., acidity absorbed during dissolution per kg product, and the reaction in soils is relatively fast with released calcium Ca considered readily available within a few weeks. Not surprising because the surface normalised dissolution rate is a factor 10^3 faster than anorthite or up to 10^7 times faster than potassium feldspar (Curtin and Smillie, 1983; Hildebrand and Schack-Kirchner, 2000; Langmuir, 1997). In both agricultural and forest ecosystems on loamy soils liming can enhance nutrient cycling and primary production (Bauhus et al., 2004; Jansone et al., 2020; Kohler et al., 2019; Moore and Ouimet, 2021; Muys et al., 2003). However, the liming of sandy soils is controversial because its fast dissolution accelerates mineralization leading to increased nitrate concentrations and carbon loss. Moreover, liming can lead to nutrient imbalances, and it promotes generalist plant species with an associated loss of specialists, i.e., calcifuge plant species (Burke and Raynal, 1998; Court et al., 2018; Hoettl and Zoettl, 1993; Kjøller and Clemmensen, 2009; Marschner and Waldemar Wilczynski, 1991; Siepel et al., 2019; West and McBride, 2005).

Therefore, the global interest is now growing in treating acid soils with silicate rock dust (RD), also denoted as rock powder/flour (Beerling et al., 2018; Kelland et al., 2020; Lewis et al., 2021; Taylor et al., 2021). Rock dust exploitation as an agricultural amendment has increased in the last decade, e.g. its share is currently pushing up to 7 % of the yearly agricultural inputs in Brazil (Manning and Theodoro, 2020; Ramos et al., 2022, 2015). Furthermore, RDs are proposed as a 'no-regret' measure on critically acidified forests to support nature restoration goals, e.g. as outlined by the Natura 2000 framework of the European Union (García-Gómez et al., 2014; Graveland et al., 1994; Jacobsen et al., 2019; van Diggelen et al., 2019; Vicca et al., 2022). Commercially, silicate RDs are a broad and not formally classified group of mining (by)products, but they are usually ground igneous or metamorphic rocks (0.001–3 mm) that consist of aluminosilicates and can contain varying amounts of other mineral classes. Among the aluminosilicates commonly found minerals in RDs are orthosilicates (e.g. olivine), inosilicates (e.g. pyroxenes such as diopside, amphiboles such as hornblende), tectosilicates (e.g. orthoclase, plagioclase, nepheline and leucite), and phyllosilicates (e.g. mica such as biotite and muscovite) (Calabrese et al., 2022; Swoboda et al., 2022; van Straaten, 2006). RDs can be an alternative to conventional liming, but in contrast to liming, they have a smaller ANC while releasing their alkalinity more gradually. In addition, they are source of a suite of nutrients such as calcium (Ca) and magnesium (Mg) but also of potassium (K), phosphorus (P), and sulfur (S) (de Vries et al., 2021; Ramos et al., 2022; Swoboda et al., 2022). Studies on RD amended soils have highlighted its potential for increased crop productivity in e.g. miscanthus (*Miscanthus* × *giganteus*), maize (*Zea mays* L.)/soybean (*Glycine max* L. Merr.) rotation, oat (*Avena sativa* L), palmarosa (*Cymbopogon martini* var. *motia*), and sorghum (*Sorghum bicolor* L. Moench) as well as increased carbon capture via increased inorganic carbon leaching or possibly through organo-mineral complexation (Basak et al., 2023; Kantola et al., 2023; Kelland et al., 2020; Ramos et al., 2015; Taylor et al., 2021).

There are hitherto, somewhat surprisingly, neither standard laboratory tests to assess the fast and slow ANC-fractions of RD nor standardized tests to identify the longevity of RD applied to soil. Hence, there is a pressing need to develop accelerated weathering tests that are simple in operation but that have predictive power for restoring acid soils (Calabrese et al., 2022; Swoboda et al., 2022). While the application of RD as a soil amendment does have to adhere environmental guidelines of mineral byproducts that can be added to soil, i.e., the products are controlled by contaminant concentrations and Ca, Mg and K content (Brazil, 2016), a standardized method to determine ANCs and dissolution rates that are relevant in soils yet has to be proposed.

Of course, the water solubility and weathering rates of silicate rocks depend on physicochemical conditions during their solidification (Bowen, 1922; Jackson and Sherman, 1953; Kronberg and Nesbitt, 1981; Wakatsuki and Rasyidin, 1992). While the mass-normalised dissolution rate increases with increasing specific surface area (SSA) (Sverdrup and Warfvinge, 1993). Also surface area-normalised dissolution rates (10^{-14}-10^{-6} mol/m^2/s) vary strongly between minerals and are a function of the pH (pH dependent slope n ~ 0.1–4), fluid composition (often measured far-from-equilibrium) and temperature (Q_{10} ~ 1.5–7) (Casey and Sposito, 1992; Gudbrandsson et al., 2011; Heřmanská et al., 2022; Langmuir, 1997).

Despite the large body of natural weathering research, e.g. studying *in situ* weathering rates and sequences (Bockheim et al., 2014; Gruber et al., 2014; White and Brantley, 2003), in contrast the dissolution rates in soils of freshly applied RD are not yet intensively studied and studies are often limited to column incubations (Gillman et al., 2002; te Pas et al., 2023). Generally, weathering rates of minerals in soils are estimated from laboratory-determined dissolution rates (Gudbrandsson et al., 2014, 2011; Hamilton et al., 2001) and from *in situ* weathering rates. Geochemists unravel these *in situ* dissolution rates by studying regoliths and perform Reactive Transport Model (RTM) simulations modelling all the processes in the Critical Zone such as geochemical reactions and diffusive, dispersive, and advective transport of solutes (e.g. PHREEQC, TOUGHREACT, MIN3P_HPC) (Anderson et al., 2002; Brantley and Lebedeva, 2011; Li et al., 2017; Strefler et al., 2018; Vienne et al., 2022). Also, soil incubations and column leaching experiments are used to validate these RTMs (Gillman et al., 2002; Hildebrand and Schack-Kirchner, 2000; te Pas et al., 2023). Ultimately all these methods serve as proxies for costly field experiments (Gruber et al., 2014; Kantola et al., 2023). Often, there is a large discrepancy in weathering rates that is attributed to the flow in natural weathering profiles having high spatial heterogeneity (Velbel, 1993; White and Brantley, 2003). This discrepancy between laboratory and field observations with discrepancy factors of 1–6 orders of magnitude depends on the mineral, study duration, and used experimental methodology (White and Brantley, 2003). Furthermore, the dissolution rates after RD application exhibit complex dynamics, i.e., a transient fast weathering pool followed by a slower weathering pool (Barral Silva et al., 2005; Hildebrand and Schack-Kirchner, 2000). Moreover, laboratory techniques such as fluidized beds, column leaching tests are time- and resource-intensive and limit the number of combinations of RD's and soils that can be tested (Cappuyns and Swennen, 2008; te Pas et al., 2023). Finally, RDs are speculated to have different dissolution behaviour depending on soil context, i.e., depending on the initial soil pH and pH buffer power, but also due to variability in clay content. The importance of these effects during RD applications have yet to be explored (Swoboda et al., 2022).

This study was set up to compare three different accelerated weathering tests for their capacity to predict the gradual liming effects of RDs in acid soils. The first of three underlying hypotheses is that the specific surface area (SSA_{BET} by N_2 sorption) and the mineralogy of the RD (by XRD) determine their dissolution rates. Second, that RD dissolution in soil depends on soil context, in casu on the actual soil pH and the pH buffer power of the receiving soil, but also on its clay content. Third, a suitable accelerated weathering test to assess RD ANC and thus predict pH increase in the soil likely reflects the rate-limiting processes in the soil, i.e., uses soil-RD mixtures. To test these three hypotheses, the dissolution rates and ANC of a range of commercial RDs were measured in three accelerated weathering experiments that increased in complexity from (1) acid consumption recording in a long-term batch renewal RD titration, up to (2) a short-term but buffered RD titration, i.e. a pH_{stat} test, towards (3) pH monitoring in agitated soil-RD suspensions. The results of these three tests were run as scenarios in a model predicting the pH increase in soils. This model was validated by a fourth experiment, a mesocosm that measured soil pH intermittently over 2 years in outdoor conditions with free drainage. Here, RDs were amended to four soil samples from Podzols and one Luvisol originating from

representative acid forests varying in texture from sand to loam.

2. Material and methods

2.1. Rock dust characterization

Five commercial rock dusts (denoted samples RD1-5) commonly applied in Europe were characterized without further fractionation by sieving. The specific surface area was determined by measuring N_2 sorption isotherms with a *Micromeritics TriStar II 3020 3.02* on 0.05 up to 0.1 g of the RD's at 77.3 K and 15 s equilibration using the Brunauer-Emmett-Teller (BET) N_2 sorption theory (Brunauer et al., 1938; McMillan and Teller, 2002). The pH was determined in 10^{-3} M $CaCl_2$ in a 1:10 w/w solid:liquid ratio after 30 min of equilibration. Total element concentrations were measured after $LiBO_2$ fusion and digestion in 50 mL HNO_3 0.42 M followed by analysis with Inductively Coupled Plasma-Optical Emission Spectroscopy (ICP-OES, *Varian 720 ES*) and dolomite (DWA-1), gabbro (MRG-1) and silica (BCS-267) were included as reference samples. The theoretical maximal ANC_{digest} (mmol/kg) was calculated from the charge-based molar concentrations of Ca^{2+}, Mg^{2+}, K^+ and Na^+ (Table S1). The mineralogy was determined via XRD-analysis after mixing with 10 wt% of an internal standard (ZnO) and milling in a wet state for 5 min in a McCrone micronizing mill. A *Philips PW1830 X-ray diffractometer* in a Bragg-Brentano setup with CuKa radiation was used, equipped with a graphite monochromator and a gas proportional detector. The operational parameters were at 45 kV and 30 mA from 5 to 65°2θ with a step size of 0.02°2θ and 2 s of scanning time per step. Quantitative mineralogical compositions were determined by processing the measured XRD patterns using Profex software for the Rietveld refinement program BGMN (Döbelin & Kleeberg, 2015). Weighted average literature-derived dissolution rates at pH 5 were calculated for each RD using the results for their mineralogical composition to weigh mineral dissolution rates found in the literature (Table S2).

2.2. Soil sampling and characterization

Four acid soils were collected in forests, more specifically two loamy sands, one sandy loam and a silt loam after attributing their particle size distribution to the following texture classes: sand (0.063–2 mm); silt (0.002–0.063 mm) and clay (<0.002 mm) (FAO Guidelines for soil description, 2006). The former three samples were collected in the 0–20 cm mineral A horizon while the latter in a previously characterized 20–40 cm depth Bt mineral horizon (Brahy et al., 2000). The first three more sandy soils (S1, S2 and S3) are Podzols originating from aeolian sand deposits in the Campine region (Beerten et al., 2014), while silt loam S4 was sampled in an Epidystric Luvisol originating from loess deposits with a siliceous nature (Brahy et al., 2000), all soils were deposited during glacial retreat in the Weichsel age (about 20 000 years BP). The critical deposition load for N in forests (15–20 kg/ha/yr) has been and still is exceeded at these sites which further degraded their buffering cation (Ca, Mg, K) balance in the past decades (e.g. for 2021: S1 = 30 kg N/ha/yr, S2 = 35 kg N/ha/yr, S3 = 28 kg N/ha/yr, S4 = 21 kg N/ha/yr). Site and soil profile descriptions are given in Table S3. The soils were sieved at 1 cm (due to the large volume) and air-dried at room temperature prior to use in the mesocosm. The soil composition is reported on oven (40 °C) dry weight basis. Soil total organic carbon and nitrogen content were determined by combustion followed by quantification with gas chromatography (GC dry combustion at 800 °C, *Thermo Isolink*) (Table S3) (Robertson, 1999). Soil pH was measured after 2 h of shaking in a 0.01 M $CaCl_2$ extract (S/L = 1 g/5 mL) with a glass pH electrode (*Metrohm*) (Schofield and Taylor, 1955). The effective cation exchange capacity (eCEC) and exchangeable cations were measured with the single step hexaminecobalt(III)chloride extraction method (Ciesielski and Sterckeman, 1997) followed by quantification with Inductively Coupled Plasma - Mass Spectrometry (ICP-MS, *Agilent 7700X*). The base saturation was calculated from the sum of equivalent charges of Ca, Mg, K and Na to the eCEC. The pH buffer power (BP_{soil}) of the soil sample (in mmol OH^-/kg soil/pH unit increase) was determined by calibrating the pH-increase of the sample at five doses of labgrade Ca $(OH)_2$ (95 %) (ANC = 25650 $mmol_c$/kg) ranging from 0.4 mg/g of soil up to 7.1 mg/ g of soil followed by 1 day equilibration in an end-over-end shaker at 30 rpm (SI Section 2, Fig. S2).

2.3. Accelerated weathering and soil mesocosm tests

Three different accelerated weathering tests were conducted to predict the soil pH rise in a fourth soil mesocosm experiment. Their duration, pH, and temperature range as well as the used number of RDs are summarized in Table 1, in all tests the treatments were full factorial combinations of start pH, temperature, and RD samples. The experiments increased in complexity, cost and/or time intensiveness.

2.3.1. Batch renewal accelerated weathering experiments

A full factorial design was set up with five RD samples, three target pH values (3.5, 4.5, 5.5), three temperatures (20 °C, 37 °C, 65 °C) and two replicates (samples = 90). For each RD, a sample of 20 g was weighed and 200 mL of 10^{-3} M $CaCl_2$ was added to mimic soil solution ionic strength. Subsequently each sample was titrated under vigorous stirring during 5 min with 1 M HCl (*certified concentration, Titrisol*) and the exact volume was recorded to restore the target pH, the added volume was maximally 35 mL at the initial fast dissolution. The jars were incubated at three different temperatures: 20 °C, 37 °C and 65 °C. The jars were titrated again after recording the start pH and at fixed times: after 4 h, 1 day, 4 days, 5 days, 17 days, 33 days and from then on at monthly intervals (# titrations = 18). At six fixed times t (after 5 days, 33 days, 90 days, 175 days, 260 days, 345 days) the solution of the jar was removed following centrifugation at RCF 5500 x g (30 min) and analysed with ICP-OES (*Thermo Scientific iCAP 7000 series*); the solutions were renewed with 200 mL 10^{-3} M $CaCl_2$ and the pH restored to the target pH. The cumulative ANC curves display a characteristic exponential shape that allows to operationally define two ANC-pools reacting at two independent first-order reactions (Schwarz et al., 1999). So, the cumulative ANC_{cum} [$mmol_c$/kg] as a function of time t [d] were fit using Equation (1) where the parameters are a fast ANC-pool ANC_{fast} [$mmol_c$/kg], a slow ANC-pool ANC_{slow} [$mmol_c$/kg], and their first order reaction constants k_{fast} [d^{-1}] and k_{slow} [d^{-1}]:

$$ANC_{cum} = ANC_{fast}\,(1 - \exp(-k_{fast}\,t)) + ANC_{slow}\,(1 - \exp(-k_{slow}\,t)) \quad (1)$$

.

2.3.2. pH_{stat} titration

Rock dust (0.1 to 0.5 g, lower in case of a larger size of the fast ANC-pool) was suspended in 200 mL of distilled water. A fast weatherable fraction was removed manually during 10–30 min of titration towards pH 3.5 by adding 0.1 M HCl equivalent to the ANC_{fast}-fraction determined in the batch renewal experiment. Subsequently, these stirred suspensions were automatically titrated (*SI Analytics™ TitroLine™ 7000 KF)* with 0.1 M HCl (a 10 x dilution of *1 M certified concentration, Titrisol*) in a pH-stat setup (3.5, 4, and 4.5) while the acid consumption rates were recorded during 0.5–3 days, the range depending on the RD and target pH to obtain a steady-state dissolution rate. A maximum 0.1 pH unit change was allowed, typically 0.03 units, between repeated HCl doses. Target pH dependent fast and slow ANC-fractions of each RD were also fitted to the cumulative ANC data using Equation (1) (Table S5). For the determination of the slope of dissolution rates with respect to pH, a steady-state surface normalised rate R_A was inferred via Equation (2) for every target pH:

$$R_w = \frac{dANC}{dt} = R_A\ SSA_{BET} = k\,ANC_{slow} \quad (2)$$

Table 1
Summary of the experimental setup for the accelerated weathering (A-C) and soil mesocosm (D) tests. The suspension test (C) used two soil samples (S3 and S4) and the mesocosm test (D) four soil samples. The pH_{stat} test was also performed at 10 °C for RD4 to derive the temperature-dependent dissolution rates.

Experiment	Time days	Start pH	Temp. °C	RD[¥] #	S/L g/mL	Cations[φ] # of times	ΔpH[€]
A) Batch	370	3.5|4.5|5.5	20|37|65	5	1/10	5	3.5
B) pH_{stat}	0.5–3	3.5|4.0|4.5	20	5	1/100	No	0.1
C) Suspension	60	3.0–3.7	20	3	1/5	No	1.5
D) Mesocosm	720	3.0–3.7	Outdoor	5		1	4

[¥] Number of rock dusts; [φ] Determination in solution (A) or exchangeable cations after hexaminecobalt(III)chloride extraction (D); [€] The maximal pH increase that was recorded during the experiment.

where R_W [mol H^+/kg/s] is the mass normalised dissolution rate, *ANC* [mol H^+/kg] the acid consumption, *t* the time [s], SSA_{BET} [m^2/kg] the specific surface area obtained by N_2 adsorption, R_A [mol H^+/m^2/s] the surface normalised dissolution rate, k the first order reaction constant [/d], and ANC_{slow} [mol/kg] the slow ANC-pool.

The surface normalised rates R_A allow to derive the slope n with respect to pH of every RD using linear regression via Equation (3) (Langmuir, 1997).

$$\log R_A = \text{-n pH} + \text{intercept} \tag{3}$$

When the slope n with respect to pH of the dissolution rate R_A is known, any rate R_A at a given pH can be extrapolated from the rate at pH 3.5 ($R_{A\ 3.5}$) by rewriting Equation (3) to obtain Equation (4). This leads to the simplification to determine *k* at a given pH using the definition of R_A from Equation (2) as shown in Equation (5).

$$R_A = R_{A\ 3.5}\left[\frac{(H^+)}{10^{-3.5}}\right]^n \tag{4}$$

$$\frac{k\ ANC_{slow}}{SSA_{BET}} = \frac{k_{3.5}\ ANC_{slow}}{SSA_{BET}}\left[\frac{(H^+)}{10^{-3.5}}\right]^n \Rightarrow k = k_{3.5}\left[\frac{(H^+)}{10^{-3.5}}\right]^n \tag{5}$$

where $k_{3.5}$ [d^{-1}] is the reaction constant at pH 3.5, ANC_{slow} [mol/kg of ANC_{slow}] the slow fraction of the ANC, SSA_{BET} [m^2/kg] the specific surface area obtained by N_2 adsorption and (H^+) the proton activity [mol/L] at which the rate is inferred.

It is noted that when using a different estimate for the ANC_{slow} in Equation (4), the reaction rate constant k also has to change to obey the fixed (and measured) rate R_A.

2.3.3. Agitated soil suspension test

A full factorial combination of soil-rock suspensions was made with three RDs (RD1, RD2 & RD4), two soils (S3 and S4) and three doses (0.045 g RD, 0.09 g RD and 0.22 g RD per 4.9 g of soil). Unamended control soils of S3 and S4 as well as soil-dolomite suspensions (0.0024 g dolomite/g soil, 0.0048 g dolomite/g soil, and 0.0121 g dolomite/g soil) were included as reference. The total number of samples totalled to 26. Soil pH was measured longitudinally in a 0.01 M $CaCl_2$ extract (S/L = 1 g/5 mL). These suspensions were shaken in an end-over-end shaker (30 rpm) at 20±1°C and pH was measured intermittently (after 2 h, 2 days, 8 days, 15 days, 22 days, 30 days, 38 days, 58 days and 289 days). The ANC of the RD [$mmol_c$/kg] was calculated via Equation (6):

$$ANC_{RD} = \frac{BP_{soil}\ \Delta pH}{dose} \tag{6}$$

where Δ *pH* is the rise in soil pH relative to the unamended control soil, BP_{soil} the pH buffer power of the soil (mmol/kg soil/ Δ pH) determined via lime-calibrated soil pH measurements and the dose expressed as kg RD/kg soil. BP_{soil} of each soil was determined via an assessment of the pH increase upon addition of $Ca(OH)_2$ in four doses: 0.0006 g $Ca(OH)_2$/g soil, 0.0012 g $Ca(OH)_2$/g soil, 0.0024 g $Ca(OH)_2$/g soil and 0.0048 g $Ca(OH)_2$/g soil (see Fig. S2). This $Ca(OH)_2$ (95 % purity) has a known ANC of 25,650 mmolc/kg. The ANC of the dolomite reference treatment measured via this method ranged 18000–22000 $mmol_c$/kg depending on the soil which approaches the theoretical value (20700 $mmol_c$/kg) thereby justifying Equation (6) for ANC determination of RD in soils.

2.3.4. Soil mesocosm experiment

Four soils were treated with five RDs in two different doses in a full factorial design with two replicates. For each dose an unamended control treatment was added (samples = 96). The RD doses were selected to reflect a tree planting pit addition in a reforested soil (high dose) or a broadcast dose (low dose). The high dose used 0.1875 g RD/g soil and corresponds to a planting pit dose of 1.5 kg RD/tree for a planting pit volume of 0.0089 m^3, it is a similar concentration of RD to a mixed broadcast dose of 340 Mg/ha for a soil depth of 0.2 m (bulk density 900 kg/m^3). The low dose used 0.0067 g RD/g soil and corresponds to 12 Mg/ha (bulk density 900 kg/m^3 and depth 0.2 m) which is common in broadcast ecosystem applications in critically N-impacted forests. The high doses were amended to 3 L pots (3 kg of soil), the low dose was amended in small columns (304 g of soil, 4.8 cm diameter, 25 cm height). Soil and RD were mixed thoroughly and incubated randomly in one of the four perforated sand boxes (1 m^2, height 40 cm) allowing free drainage and installed outside on a building rooftop safe from animal interventions in Leuven in March 2021 (SI section 9c). Soil pH was measured in 0.01 M $CaCl_2$ extract (S/L = 1 g/5 mL) after eight months, after 15 months and after 24 months. Total precipitation during that period was 1600 mm, sufficient for cumulative leaching of 32 (small columns) or 40 (larger pots) pore volumes. The eCEC and base saturation were determined after eight months using the hexaminecobalt(III) extraction protocol (Ciesielski et al., 1997).

2.4. pH-dependent weathering model

The soil pH increase of the soil mesocosm experiment was modelled using the accelerated laboratory tests. As a first step, the soil pH values measured via standard 0.01 M $CaCl_2$ extractions were corrected as small uncertainties in pH largely affect the model evaluation. It is well established that the pH of soils with variable negative charge decreases with increasing ionic strength (IS) of the solution. The IS of the soil solution in the mesocosms is likely lower than that in the 0.01 M $CaCl_2$ extract (30 mM) as the soils are aged with free drainage and not fertilised. Moreover, the IS likely depends on the treatments as organic matter mineralisation and nitrification rates markedly increase as soil pH rises (Curtin and Smillie, 1983). Indeed, the IS, detected via electrical conductivity (EC) of water extracts of amended soils, confirmed the *in situ* IS of rock dust treated soils varied with the rock dust treatments, they were lowest for the unamended control soils (0.5–6.0 mM) and reached up to 25 mM in RD treated ones. Hence, the pH of each soil sample was corrected for *in situ* IS (SI section 7). This pH adjustment was on average a 0.3 unit increase compared to the measured pH in 0.01 M $CaCl_2$. The corrected pH values are referred to as *soil pH* in the modelling results section of the paper.

In the second step, the proposed model to predict the pH increase as a function of RD parameters and soil parameters is based on Equations (1)

and (5) simplified by the assumption that the fast pool of ANC reacts instantaneously and that the slow pool weathers at a rate controlled by the pH. The numerical integration of the rate equations and mass balance reads to Equations (7):

$$\Delta pH_0 = ANC_{fast}\frac{Dose}{BP_{soil}}$$

$$\Delta pH_i = \Delta pH_{i-1} + \left\{\frac{Dose}{BP_{soil}}\, ANC_{slow,i-1} k_{3.5}\left[\frac{(H^+)}{10^{-3.5}}\right]^n\right\}(t_i - t_{i-1})$$

$$ANC_{slow,i} = ANC_{slow,i\text{-}1}\left\{ ANC_{slow,i\text{-}1} k_{3.5}\left[\frac{(H^+)}{10^{-3.5}}\right]^n\right\}(t_i\text{-}t_{i\text{-}1}) \quad (7)$$

in which ΔpH_i is the pH increase relative to the previously modelled pH_{i-1} and the modelled soil pH at time t_{i-1} is $pH_{start} + \Delta pH_0 + \ldots + \Delta pH_{i-1}$, ANC_{fast} [mol H^+/kg RD] is the fast fraction of the ANC measured in the pH_{stat} experiment, dose [kg RD/kg soil] is the applied RD dose, BP_{soil} [mol H^+/kg soil / Δ pH] is the pH buffer power, ANC_{slow} [mol H^+/kg RD] is the slowly available fraction of the ANC determined by the screening tests, $k_{3.5}$ [/day] is the measured rate of weathering for each RD in the pH_{stat} experiment, (H^+) [mol/L] is the proton concentration actualized by the modelled soil pH value, n [-] is the slope of the weathering rate with respect to (H^+) and t_i [days] is the modelled time. The first modelled time interval t_1 was 0.1 day and was increased for every step as: $t_i = 1.1\ t_{i-1}$.

2.5. Statistical analysis

All analyses were executed with R 4.0.5 (Rdc, 2009). Linear (mixed) models were constructed to test for significant differences in soil variables between RDs, or to regress modelled vs measured pH using the package *lme4* (Bates et al., 2014). The cumulative ANC of all treatments and time points was analysed with linear mixed models (Cumulative ANC ~ Time x RD type x Target pH x Temperature) with sample ID as a random intercept effect. Post-hoc pairwise comparison tests (Tukey or Dunnett's test) were used to test within-treatment significance, by using package *lsmeans* (Lenth, 2016). Nonlinear least squares regression models were used for the two pool parallel power model fits of cumulative ANC as a function of time using the package *stats* (Bates and Watts, 1988). Colourblind and grey scale friendly graphs were build using the packages *ggplot2* and *viridis* (Garnier et al., 2021; Wickham, 2011). All trends and differences were only mentioned after hypothesis testing and levels of significance $p < 0.05$.

3. Results

3.1. Properties of rock dust and soil samples

Selected properties of the RD samples are summarised in Table 2. The SSA_{BET} ranges between 0.3–5.5 m^2/g with the highest value for RD1 which is a phonolite rock that contains some zeolite and lime. All materials are alkaline with pH values 8.7–9.2 measured in 0.01 M $CaCl_2$. The range in maximal ANC values, derived from digestion, is equivalent to 20–50 % of the ANC of calcite. The XRD results illustrate (Fig. S1) that the RD are mainly composed of diopside, plagioclases and K-feldspars for RD2, RD3 and RD4 with varying amounts of nepheline. RD5 also contains muscovite and chlorite while RD1 is a mixture of fast weathering minerals (calcite, natrolite) and slow weathering minerals (K-feldspars). A theoretical ranking of the dissolution rates of the five RD samples was derived from literature based mineral dissolution rates at pH 5 that were weighted in proportion to XRD based mineralogical fractions and corrected for the SSA of the samples (Table S2). These weight based corrected theoretical dissolution rates at pH 5 vary factor 10, the lowest ranked sample is RD4 with smallest SSA (most coarse particles), the higher ranked sample RD2 is the phonolite based one that has the highest SSA combined with fast dissolving minerals.

Chemical properties of the four soil samples used in the suspension and mesocosms are given in Table 3. All samples are acid (pH < 3.7) with less than 20 % base saturation. The pH buffer power increases with increasing eCEC values of the soil, indicating that the pH buffer is largely controlled by cation exchange reactions. Evidently, the cation exchange complex of A horizons S1 (2.1 % C, 1.6 % clay), S2 (3.3 % C, 2.5 % clay) and S3 (3.7 % C, 2.8 % clay) are characterized by OM-dominated charge while the Bt horizon in S4 (0.4 % C, 9 % clay) has its cation exchange complex dominated by clay-derived charge (Table S3).

3.2. Batch renewal accelerated weathering experiment

Fig. 1 shows the cumulative ANC on one of the five RD samples, trends for the remaining RD samples were similar (Fig. S3). The pH largely fluctuated between two consecutive titrations with amplitudes up to 3 pH units at the start of the experiment (Fig. 1, top). The ANC dynamics under these non-steady state conditions reveal, as expected, a rapidly reacting fine fraction followed by a slow ANC fraction. The significant fixed effects of the linear mixed model explaining cumulative ANC were RD type, time and target pH (all $p < 0.0001$), but effects of temperature were small and inconsistent ($p = 0.66$).

The dynamics of the cumulative ANC through time (Fig. 1)) can be better described by a parallel two-pool first order dissolution model, i.e., by Equation (1). The fitted parameters for the five products can be found in Table S4, the graphs of the other RDs are supplemented (Fig. S3). The half-lives of the fast pools ($\ln 2/k_{fast}$) are all <1 day and for the slow

Table 2
Selected rock dust (RD) properties, RDs are ranked according to their total Acid Neutralising Capacity (ANC).

Product	Classification	Origin	SSA_{BET} [£] m^2/g	pH_{CaCl2} [¥]	ANC_{digest} [φ] $mmol_c/kg$
RD1	Basalt	DE	3.0	9.2	10 400
RD2	Phonolite[x]	DE	5.5	9.1	8 300
RD3	Basalt	DE	1.8	8.7	7 800
RD4	Foidite	NO	0.3	9.0	7 300
RD5	Trachy-andesite	AT	3.1	9.0	4 300
Lime	Dolomite	BE	/	/	20 700

[x] Phonolite sample also contained a zeolite mineral, i.e. natrolite as well as some calcite (see Table S2).
[£] Specific surface area (SSA_{BET}) with N_2 adsorption and BET theory.
[¥] pH in 1 mM $CaCl_2$ at 1:10 soil:liquid ratio (30 min equilibration).
[φ] Total ANC concentration determined by digestion with $LiBO_2$ of the buffering cations Ca^{2+}, Mg^{2+}, K^+ and Na^+ with acid neutralising capacity.

Table 3
Selected properties for the soil samples.

Soil	Texture	pH_{CaCl2} [£]	eCEC[¥] $cmol_c/kg$	BS [φ] %	$BP^{€}_{soil}$ mmol OH^-/kg soil/ ΔpH
S1	Loamy sand	3.5	1.9	18	23
S2	Loamy sand	3.2	2.7	10	30
S3	Sandy loam	3.1	3.3	11	33
S4	Silt loam	3.7	6.1	14	39

[£]pH in 10 mM $CaCl_2$ at 1:5 (5 g/ 25 mL) soil:liquid ratio (2 h equilibration); [¥] cobalthexaminechloride method [φ] Base saturation [€] pH buffer power of soils determined in lime titrated soil suspensions.

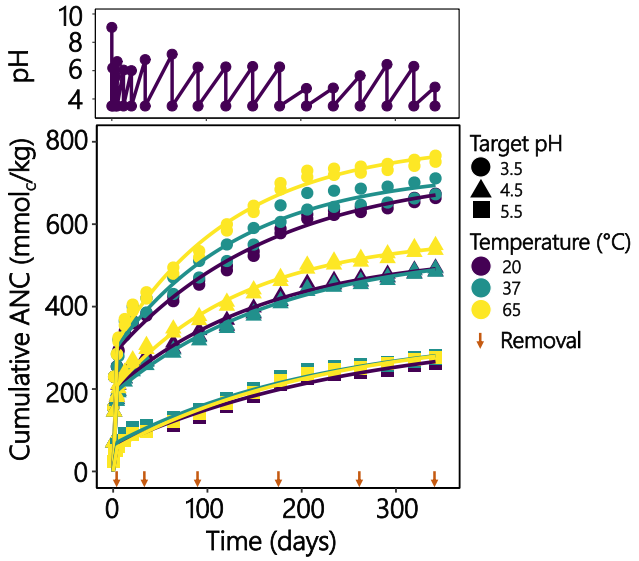

Fig. 1. Results of the batch renewal weathering tests: cumulative acid neutralising capacity for rock dust sample RD4. The target pH is indicated by the shape, incubation temperature is indicated by colour. The curves are fits of the two-pool first order power model from Equation (1). Removal and renewal of the solution is indicated by brown arrows on the time-axis. The upper plot shows the evolution of the pH during the experiment for the case of target pH = 3.5 and T = 20 °C.

pools ranged between 60 and 230 days. The RD products differ largely in ANC_{fast}-pool sizes, that pool was highest for RD1 and RD5. These RD contained significant amounts of calcite and dolomite respectively. The size of ANC_{slow} and the dissolution rate constants are not further discussed because the non-steady state pH (i.e. fast pH increase) reduces the dissolution rates in these batch experiments and these are, therefore, underestimated when compared to the ANC_{slow} measured in the two accelerated weathering tests described below.

The cumulative release of cations to the solution, i.e. the sum of equivalent charges of Ca, Mg, K, Na, Al, Fe and Mn, was plotted to the titration data, i.e. the cumulative ANC. That plot shows a linear relation (Fig. S4) with a very high correlation (R^2 = 0.997) and a slope (1.01) that corresponds markedly well to the 1:1 line confirming the validity of the titration results. The main pH neutral cations used for pH buffering in soil are Ca^{2+}, Mg^{2+}, Na^+ and K^+, often termed base cations in soil chemistry. These base cations constitute between 60 and 90 % of the cumulative released charge-based cations, the range depending on the RD and the respective cation pulses depending on mineral stability (Fig. S5). Initially mostly Ca, and Mg are released followed by pulses of Al, K and Na. Further analyses of the dissolved elements are made in SI Section 3, drawing attention to the remarkable high proportion of Al-release for the basalts RD1 & RD3.

Table 5
Acid neutralising capacities (ANC) of rock dusts and dolomite inferred from total elemental analysis (ANC digestion) and from the four weathering tests, all at the lowest (starting) pH 3.5. The ANC digestion is the sum of charge-based buffering cations Ca^{2+}, Mg^{2+}, K^+ and Na^+ The ANC derived from the batch renewal, pH_{stat} and suspension tests are fitted with Equation (1) and are the sum of the fitted slow and fast fraction, the ANC of the mesocosm is based on the difference in soil pH between amended and unamended soil at the end of the test (720 days) and converted to the ANC with the pH buffer power of the soil that, in turn, was derived from soil titration in the laboratory.

	ANC				
	Batch	**pH_{stat}**	**Soilsusp**	**Mesocosm**	**Digestion**
Start pH	3.5	3.5	3.1	3.1–3.7	
Duration (days)	360	1	60	730	
			$mmol_c$/kg		
RD1 Basalt	500	2300	3400	1800	10 350
RD2 Phonolite	4500	10 500	5300	2200	8300
RD3 Basalt	600	800	/	800	7800
RD4 Foidite	750	2900	3100	1500	7300
RD5 Trachy-andesite	1200	1600	/	400	4300
$Ca_{0.5}Mg_{0.5}CO_3$	/	/	17 300	10 300	20 700

3.3. pH_{stat} titration

Table 4 yields the steady state dissolution rates of the RD samples for different set pH values. These rates refer to dissolution of the slow fraction of the products because the fast ANC fraction was removed by manual acidification before titration started. The dissolution rates are only recorded once steady state titration rates were obtained. The dissolution rates (R_{meas}) decrease factors 10–100 between pH 3.5 and 4.5, regression lines between $logR_{meas}$ and pH have R^2 values > 0.9 and slopes (n) range between 1 and 2 depending on the RD type (Table 4). RD2 phonolite, RD4 foidite and RD5 trachy-andesite have a lower slope (n ~ 1) than basalts RD1 & RD3 (n ~ 2). The basalts also had notably higher charge-based aluminium (Al) contribution to the ANC (Fig. S5). With one exception, measured dissolution rates (R_A), corrected to pH = 5.0 are below corresponding literature derived rates (R_{lit}) (Heřmanská et al., 2022; Knauss et al., 1993; Langmuir, 1997; Lasaga et al., 1994; Lewis et al., 2021), however the ranking among RDs was rather consistent. The dissolution rate for basalts and trachy-andesite specifically are lower than the literature-derived rate while for the foidite (coarsest product, lowest SSA_{BET}) the measured rates are 3-fold larger than the literature-derived rates. The pH_{stat} data were combined with the initially removed ANC to obtain cumulative ANC versus time that was fitted with Equation (1). The rate constants and pool sizes of the ANC_{fast} and ANC_{slow} fractions are given in Fig. S6 and Table S5. The first order dissolution rate constants k_{fast} and k_{slow} were about a factor 10–100 times faster than in the batch renewal experiment, confirming

Table 4
Results of pH_{stat} titration: measured rock dust dissolution rates (R_A) at three target pH values. The dissolution rates refer to steady state rates obtained after first removing the fast fraction of the ANC pool, hence these rates refer to those of the slow fraction. The rates decrease with increasing pH and the slope n of the regression line between $logR_A$ and pH is given with its standard error (SE). The R_A is extrapolated to pH 5 with the slope n and is compared to the mineralogy and literature-derived rates (R_{lit}) given in Table S2.

RD	R_A pH 3.5 mol/m²/s	R_A pH 4.0 mol/m²/s	pH 4.5	n (SE)	R_A pH 5 mol/m²/s	R_{lit} mol/m²/s	R_A/R_{lit}
RD1 Basalt	$8.7\ 10^{-9}$	$1.4\ 10^{-9}$	$8.1\ 10^{-11}$	−2.0 (0.3)	$9.3\ 10^{-12}$	$3.5\ 10^{-10}$	0.03
RD2 Phonolite	$9.9\ 10^{-9}$	$1.7\ 10^{-9}$	$9.9\ 10^{-10}$	−1.0 (0.3)	$3.1\ 10^{-10}$	$5.1\ 10^{-10}$	0.62
RD3 Basalt	$8.9\ 10^{-9}$	$1.1\ 10^{-9}$	$1.0\ 10^{-10}$	−1.9 (0.1)	$1.2\ 10^{-11}$	$2.7\ 10^{-10}$	0.04
RD4 Foidite	$1.1\ 10^{-7}$	$3.3\ 10^{-8}$	$7.1\ 10^{-9}$	−1.2 (0.1)	$1.9\ 10^{-9}$	$7.1\ 10^{-10}$	2.72
RD5 Trachy-andesite	$7.2\ 10^{-10}$	$2.2\ 10^{-10}$	$5.5\ 10^{-11}$	−1.1 (0.05)	$1.6\ 10^{-11}$	$1.4\ 10^{-10}$	0.11

that the renewal test largely underestimates dissolution rates due to the non-steady state conditions in that renewal test. Along the same line, the total ANCs, determined by pH_{stat} were consistently larger than those in the batch renewal test (Table 5). For one sample (RD4), the pH_{stat} dissolution rates were measured at two temperatures (10 °C and 20 °C) yielding a Q_{10} of weathering for the slow pool of 1.6, details are given in SI, section 4.

3.4. Agitated soil-RD suspension test

In the agitated soil-RD suspensions an initial fast pH increase was followed by a slower increase around pH 4–4.5 that halted already after 60 days (Fig. 2). The corresponding ANCs calculated with the soil pH buffer power via Equation (6) are about 4–5 times higher than corresponding values in the batch renewal experiment after 30 days at the lowest starting pH for RD1 and RD4 but correspond well for the quickly dissolving sample RD2. The ANC is clearly larger as the initial soil pH is lower on the sandy A horizon soil sample (S3), while it is lower on the loamy Bt horizon sample (S4) with higher initial soil pH (Fig. 2). Furthermore, increasing doses of RD yielded higher pH values but decreasing return in final ANC of the RD (SI section 5, Figs. S7 and S8).

3.5. Soil mesocosm experiment

During the outdoor incubations, vegetation started to grow from the seedbank in the soil in the largest pots with highest RD doses. The treatments markedly affected the vegetation cover, with almost zero cover in all four acid soils in contrast with near full cover in the soils amended with RD, e.g. most pronounced with RD1 phonolite (SI Section 9c). Soil pH significantly increased after addition of RDs (Fig. 3). At the low dose of 12 Mg/ha, the rise in pH was largest for RDs with the largest ANC_{digest} while for RDs with similar ANC_{digest} the ranking of pH increase can be made with the ranking of dissolution rates derived from literature or from the pH_{stat} experiment. Smaller pH increases are observed as soil CEC increases in the sequence of S1 to S4, however the ANC of RDs in S1 and S4 are similar despite the textural difference. The corresponding ANCs are lower than those found in the soil-RD suspension test. At the high dose of 340 Mg/ha, pH increases are larger than at the low dose (SI section 6). The largest soil pH values up to pH 6–7 were reached with RD2, RD4 and RD5 that had least pH dependent dissolution rates, i.e., a small slope n. Whereas high slope n RDs, e.g. basalt based RD1 & RD3, did not yield such high pH increases as soil pH stabilized around 5 (Fig. S9 and Table S6).

3.6. pH-dependent modelling

The model's input parameters for ANC_{fast} and ANC_{slow} derived from the three laboratory tests are given in Table 6 and are referred to as those of three modelling scenarios. Scenario A uses the data of the batch-renewal tests at 20 °C and starting pH = 3.5, ANC_{slow} is the difference between the total ANC_{digest} and the ANC_{fast} pool under these conditions. Scenario B uses the pH_{stat} test data at 20 °C at the lowest pH = 3.5. Scenario C uses the parameters from the suspension test (20 °C, only most acid soil S3) and is more limited as it only used three of the five RDs (Table 6). All slow pool dissolution rates were consistently derived from the pH_{stat} data at pH = 3.5 but the rate constant $k_{3.5}$ was adjusted for each of the three scenarios to obtain equal dissolution rates R_W depending on the ANC_{slow} used in that scenario $R_w = k_{3.5}\ ANC_{slow}$, see Equation (2). All rate constants were corrected with Equation (8) (SI section 4) for temperature assuming that the mean soil temperature in the mesocosms was 10 °C and that the Q_{10} is 1.6 as found in the pH_{stat} test.

The fitted pH values were regressed against the measured pH values at the three sampling times of the mesocosm (t = 240, 450 and 720 days) and for three scenarios (Fig. 4). For the low dose, the (A) scenario overestimates the measured soil pH by, on average 0.5 (standard deviation 0.3) pH units. Modelling with the ANC fractions from the pH_{stat} experiment (B) partly resolves this overestimation but the prediction power ($R^2_a = 0.37$) is significantly lower than in scenario (A). Finally, the suspension test (scenario (C)) is superior in predicting outdoor soil pH

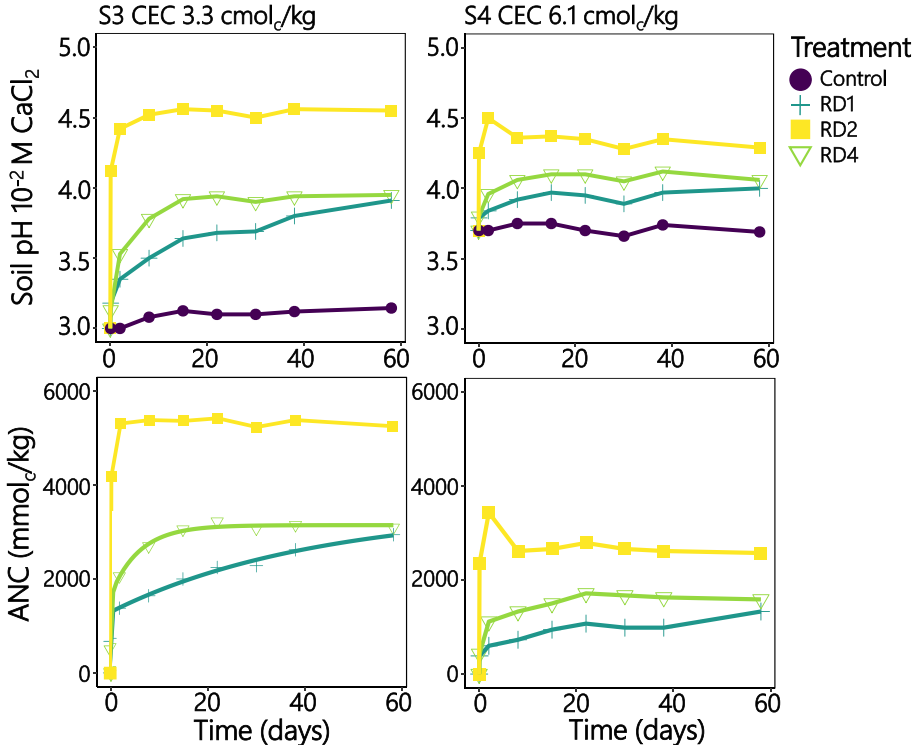

Fig. 2. Soil pH measured in agitated soil suspensions (upper panel) of three RDs dosed at 9.1 mg RD/g soil for two soils (S3 left and S4 right) and calculated corresponding RD ANC from the soils buffer power (lower panel). The graph illustrates the larger ANC for RD used on soil S3 with a lower initial pH.

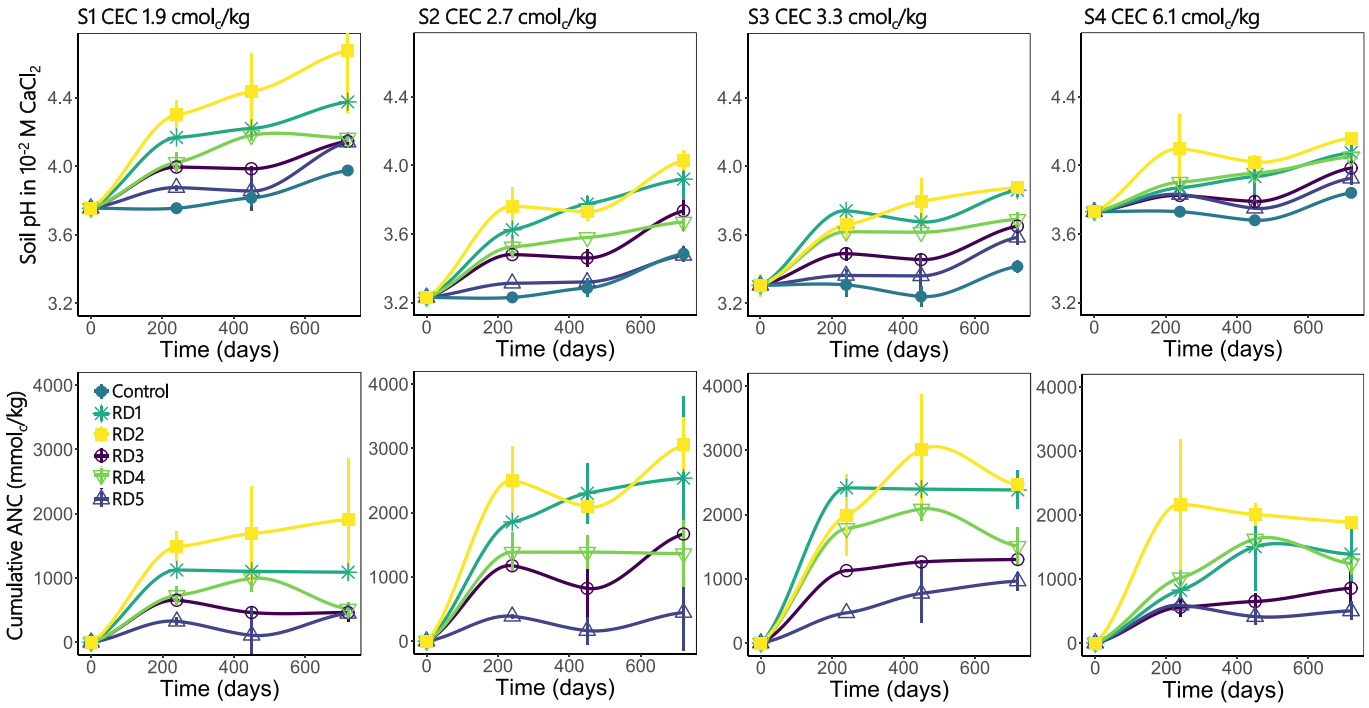

Fig. 3. The trend in soil pH in the mesocosm experiment showing means and 95 % CI (upper panel) and corresponding calculated RD ANC (lower panel) for six treatments (shapes), four different soil samples (panels left to right) and the low dose (0.0067 g RD/ g soil ~ 12 Mg/ha).

Table 6
ANC input parameters for the three scenarios of the pH-dependent weathering model at two RD doses. For the low dose, scenario (A) uses the fitted ANC_{fast} from the batch renewal test and $ANC_{slow} = ANC_{digest} - ANC_{fast}$. Scenario (B) uses ANC_{fast} and ANC_{slow} fits from the pH_{stat} experiment while scenario (C) uses the fits from the suspension test on S3. Each scenario's $k_{3.5}$ constants are derived from normalised pH_{stat} measured weathering rates at pH 3.5 that were calculated relative to the fraction of the scenario's respective ANC_{slow} fraction (A), (B) or (C) in the RD. The high dose uses the same estimation methodology of ANC but because pH increased quickly above pH 5 it is assumed that the ANC_{fast} is significantly smaller due to lowered solubility at elevated pH. To model this high dose we therefore included all ANC_{fast} as ANC_{slow} and recomputed the $k_{3.5}$ constants.

	ANC_{fast}			ANC_{slow}		
	(A) Batch	(B) pH_{stat} $mmol_c$/kg	(C) Susp	(A) Digest	(B) pH_{stat} $mmol_c$/kg	(C) Susp
Low dose						
RD1	350	900	1200	10 000	1400	2200
RD2	3900	3700	4000	4400	6400	1300
RD3	320	300	–	6600	540	–
RD4	290	600	1600	7000	2300	1500
RD5	1000	1300	–	3300	300	–
High dose						
RD1	0	0	0	10 350	2300	3400
RD2	0	0	0	8300	10 100	5300
RD3	0	0	–	6920	840	–
RD4	0	0	0	7290	2900	3100
RD5	0	0	–	4300	1600	–

due to higher precision and accuracy ($R^2_a = 0.67$ and RMSE = 0.29).

4. Discussion

4.1. Relationship between rock dust weathering, its mineralogy and specific surface area

The instantaneous pH increase and the corresponding fast ANC fraction was largest for RD2 & RD5 that contained dolomite or calcite or had the largest specific surface areas (SSA_{BET}) confirming the importance of grinding to the ANC of a RD (Swoboda et al., 2022). The slow ANC-fraction weathering rates at pH 5 derived from pH_{stat} titrations varied between 10^{-9} and 10^{-11} mol/m^2/s and ranked RD's in the same order as literature-derived rates (Tables 4 and S2). The proven correlation and similar ranking of RDs for these literature and experimental rates confirms the major importance of RD mineral composition with respect to weathering rates (Langmuir, 1997).

The SSA was less affecting the slow pool dissolution rates than those of the fast pool. For example, RD4 (SSA_{BET} ~ 0.3 m^2/g) which had particles mostly above 100 μm in size, did weather significantly faster than expected from surface normalised weathering rates and even faster than some RD's with 10-fold higher SSA_{BET}. This suggests that for some minerals, finer grinding would not affect long-term weathering. Indeed, it is known that during weathering particles decrease in size which drastically increases their SSA_{BET} (White and Brantley, 2003). Further experimental study on the importance of grinding intensity is needed as this result contradicts current model simulations (Rinder and von Hagke, 2021). Furthermore, surface normalized rates could have little relevance for certain minerals found in RD4 (e.g. micas), since its reactive sites can be concentrated on edge surfaces which only comprise a minor fraction of the total surface area (Kalinowski and Schweda, 1996).

The slow ANC fractions of RDs range between 500 and 3000 $mmol_c$/kg (Table 6), evidently lower than the theoretical 20 000 $mmol_c$/kg of calcite, and dependent on minerals such as nepheline, anorthite, diopside, hornblende (Table S2). Indeed, RD1 basalt and RD4 foidite are rich in these minerals and showed most gradual weathering upon addition to soils as reflected in the sustainable increases in soil pH from 3 up to 5 in a less-aggressive way than lime. Therefore, RD's containing these moderately slow dissolving minerals have a high potential for use on acidified soils due to their gradual but effective dissolution rates (Figs. 2 and S6). In contrast, the phonolite RD2, basalt RD3, and trachy-andesite (RD5) contain clays, quartz, albite or K-feldspars and have very small (RD3) up to negligeable (RD2 and RD5) slow-release liming properties too after depletion of their fast ANC-fraction.

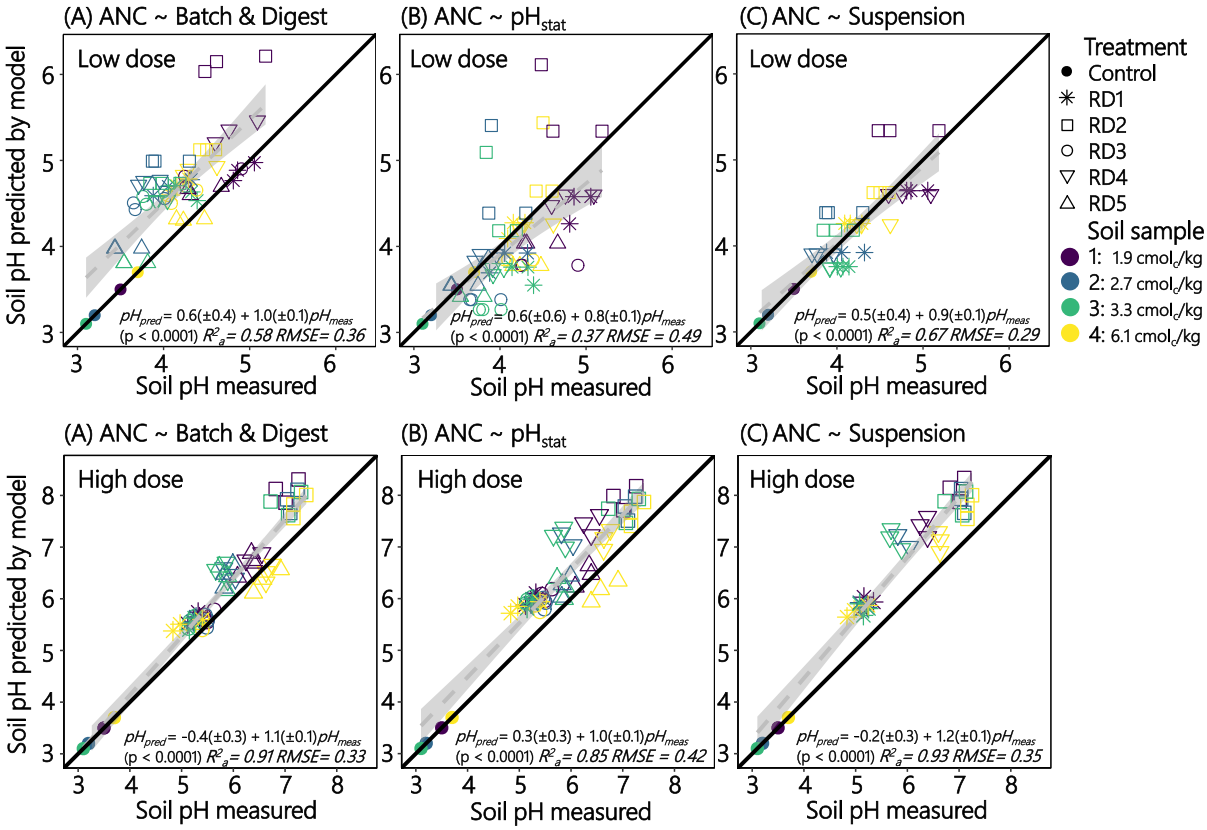

Fig. 4. Predicted versus measured soil pH for four different soils (colours), six treatments (shapes) and two doses (upper and lower panels, the 1:1 line is indicated with a solid line. For the low dose (12 Mg/ha), the pH-dependent slow pool model overestimates the soil pH measured in the mesocosm experiment for all measuring times (t = 240 days, t = 450 days and t = 720 days) when the ANC_{slow} is assumed equal to the ANC_{digest} minus the ANC_{fast} from the batch renewal test (A). Modelling with the ANC fractions from the pH_{stat} experiment (B) or the suspension test (C) resolves this overestimation. Also for the high dose (340 Mg/ha), the measured rates R_A and slope n with respect to pH effectively rank soil pH outcomes.

The pH-dependency of weathering rates of RDs decreased drastically with increasing pH in the pH range 3.5–5.5. The rates follow about first (n = 1) up to second (n = 2) order reaction kinetics with respect to pH (Table 4). Experimental slopes in the literature vary between 0.2 and 1.6 for pure minerals, making our findings for the basalts (n ~ 2) on the higher end (Blum and Lasaga, 1988; Heřmanská et al., 2022; Knauss et al., 1993). The RD2, RD4 & RD5 thus follow the logical trend of slopes such as found for its minerals nepheline (n = 1), hornblende (n = 0.7), and biotite (n = 0.6) (Hamilton et al., 2001; Kalinowski and Schweda, 1996; Zhang et al., 1996). The high pH-dependency for basalts RD1 & RD3 was also confirmed in the suspension and mesocosm tests at elevated RD dose of 340 Mg/ha for which the soil pH did not even increase above 5 (Table S6). These larger slopes with respect to pH for basalts RD1 & RD3 is likely related to the dissolution of anorthite $CaAl_2Si_2O_8$ (n = 4) in RD3 and leucite $KAlSi_2O_6$ in RD1 (Amrhein and Suarez, 1988). These minerals have large slopes due to the dissolution of high charge cations in initial weathering stages. Indeed, specifically aluminium contributed up to 50 % on a charge basis to the ANC at pH 3.5 but did not dissolve at pH 4.5 for RD1 & RD3 (Fig. S5). Pure $Al(OH)_3$ dissolves at low pH as: $Al(OH)_3 + 3H^+ \rightleftharpoons Al^{3+} + 3H_2O$, this leads to a reaction rate equation proportional to its surface speciation of $R \sim k(H^+)^3$ (Blum and Lasaga, 1988). At higher pH, dissolved aluminium could even precipitate on the surface of RD particles, this surface passivation could further slow down dissolution rates (Calabrese et al., 2022; Daval et al., 2018; Knauss et al., 1993).

Practically, this large pH-dependency of RD dissolution rates has an advantage that aggressive pH increases are avoided, e.g. they are safer to apply in large doses because of the smaller probability of overdosing, an aspect that may be most relevant for restoring buffering cation deficient ecosystems sensitive to aggressive changes. For agriculture, in contrast, liming to pH neutral condition may be desirable and RD's that also weather at elevated soil pH such as RD2 phonolite and RD4 foidite may be more promising (Fig. S7) or mixtures of RDs with agricultural lime should be explored.

4.2. *Comparing the ANC of RDs among laboratory tests, mesocosm, and soils*

The total ANC at a starting pH near 3.5 (Table 5) for the five RDs and dolomite were compared among the four experiments and compared with the ANC derived from total cations Ca, Mg, K and Na, the latter termed the ANC_{digest}. The ANC in batch renewal tests were clearly lower than in all other tests, illustrating that the periodic rise in pH and soluble cations underestimated weathering in the other systems, including soils. The ANC_{digest} was never reached in any test but was most closely approached in the pH_{stat} test and soil suspension of the most acid soil where solution pH was most buffered and cation concentration in solution either buffered by ion exchange reaction or low due to a low RD/water ratio (pH_{stat}). The mesocosm test of the most acid soil yielded lower ANC than the suspension test, despite longer exposure times, and this was even the case for dolomite. This may suggest that mass transfer limits weathering in soil and/or that temperature effects are at stake.

All buffered laboratory tests showed good agreement in the ranking of RD dissolution rates at pH 4.5: RD2 phonolite > RD4 foidite > RD1 basalt > RD3 basalt > RD5 trachy-andesite. However, in the soil mesocosm, the low initial soil pH resulted in a proportionally higher increase in basalt dissolution rates (n ~ 2) compared to the other RDs (n ~ 1), changing the ranking to RD2 phonolite > RD1 basalt > RD4 foidite >

RD3 basalt > RD5 trachy-andesite.

Generally, weathering is promoted by decreasing pH and by increasing pH buffer power of the soil (BP_{soil}). The BP_{soil} is a measure for the amount of acidity a unit of soil absorbs for unit pH change and depends on the soil carbon and clay content. The BP_{soil} is therefore a concept that is successfully adopted here from liming practices (Aitken et al., 1990). In the soil suspension experiment, RD weathering is driven by soil acidity, leading to a soil pH- and dose-dependent ANC of RDs; meaning that lower ANCs are found for higher initial soil pH and higher doses (Fig. S7). The dissolution rates in the suspension experiment also halted in the pH range of 4.5–5.5, likely due to equilibria and surface limitations of slow ANC-fraction dissolution. Possible explanations are, on the one hand, that excess solute concentration retards the dissolution reactions by increasing ionic strength IS (>30 mM) (Oelkers et al., 1994). On the other hand, the reduced weathering rates may relate to surface passivation of the RDs by a layer of precipitated secondary minerals (Daval et al., 2018).

The agitated soil suspension data (Fig. 2) show ANCs are lower when tested in the low organic matter soil sample of the Bt horizon (S4) than corresponding values in the sandy and organic matter rich sample S3 from the A horizon. When re-examining ANCs between S2, S3 and S4 in the mesocosm data (Fig. 3), this is also observed albeit more minor. Next to a merely actual pH-related effect we have to highlight that in the sandy soils (S1, S2, S3) most of the exchange reactions involve the titratability of OM. While the minerals in the clay fraction from the Bt horizon (S4) are smectite, mica, kaolinite, quartz and interstratified 2:1 minerals (Brahy et al., 2020). Due to the nature of these minerals their titratability is likely posing issues to desorb highly charged cations like Al^{3+} around pH 4.5, thereby retarding further RD dissolution which could explain the related lowered ANC measured for RDs on this soil S4. For example, kaolinite has a high affinity for aluminium ions (Walker et al., 1988). So the organic matter in the sandy A horizons could have released its Al^{3+} more easily, following the phenomenon that is known to trouble the pH restoration in soils with higher clay content (Chadwick and Chorover, 2001; Vitousek and Chadwick, 2013).

All these mechanisms, indeed, become dominant in the pH range 4.5–5.5 and can explain why the weathering rate in soil suspension was slower than in the pH_{stat} experiment despite the similar solution pH (Chadwick and Chorover, 2001).

4.3. Predicting gradual pH increases to determine the best accelerated weathering test

The accelerated RD weathering tests were set up to identify which test could predict the RD weathering rates in real world acid soils, i.e. the pH trends in the soil mesocosms. This section will deal with this modelling. At the outset is the use of Equation (1) that calculates the ANC of the products as a function of weathering time, the weathering rate constants and the slow and fast fraction. The key question is which of the three accelerated weathering tests yields most adequate model parameters to predict the data of the mesocosm.

The fitted pH values were regressed against the measured pH values at the three sampling times of the mesocosm (t = 240, 450 and 720 days) and for three scenarios (Fig. 4). This analysis using RD variables (ANC_{fast}, ANC_{slow}, SSA_{BET}, k and n) as well as soil variables (in situ pH and BP_{soil}) showed satisfactory predictions that differed amongst laboratory scenarios. The (A) scenario overestimates the measured soil pH by, on average 0.5 pH units. Hence as expected, the ANC of the digest overestimates the ANC as it assumes that cations from poorly soluble K-feldspars, albite and even clay-minerals contribute to ANC. Modelling with the ANC fractions from the pH_{stat} experiment (B) partly resolved this overestimation but the suspension test (scenario (C)) is superior in predicting outdoor soil pH due improved precision and accuracy. So the analyses suggest that, at realistic broadcast doses, the slow-release liming properties of RD's in soil are most successfully predicted by combining an (1) agitated soil suspension test to infer the ANC fractions and (2) a pH_{stat} titration at pH = 3.5 and 4.5 to infer the weathering rate of the slow fraction and its pH dependency (Fig. 4). The validated model can be used to infer environmentally relevant trends such as the half-life of the ANC_{slow}. For example, in the most acid soil S1 starting at pH 3.5, the half-lives of the ANC_{slow}-fractions are less than 5 days while at the agriculturally relevant starting pH of 5.5, half-lives range 130 days (RD4) up to 130 years (RD1). The very short half-lives in the acid soils are probably underestimated and cannot be validated as no short-term contact studies were performed on the mesocosm. Future studies with agricultural soils that are higher in initial pH and pH buffer power should be included to verify these rate predictions. However, for the high dose the model also showed good soil pH predictions (Fig. 4) thereby emphasizing the major influence of the pH-dependent rate contants k, i.e., of the slope n.

It is proposed based on these results that for ultra-acid soils (pH < 3.5) for which there is no need to prevent quick pH increases, liming may be a better option for the initial pH increase because RD weathers also quite fast at these pH values. However, to buffer the pH in the strongly acid pH range (pH 3.5–5), RDs effectively act as slow-release lime. Above pH 5, RDs differ significantly in their action, largely determined by their pH-dependent dissolution rates. For loamy soils, i.e., with a higher pH buffer power, it could still be relevant to amend RD at elevated pH > 5 with small slope n as the pH is buffered well by the soil, while for sandy soils, i.e. with lower pH buffer power, it is likely better to optimize the dose or choose a RD with a large slope n to prevent pH overshoot. This is how in practice choices on amendments and doses can be made based on soil type/chemistry and RD geochemistry.

The challenge of assessing transport-limited dissolution rates (Calabrese et al., 2022) was circumvented by well mixing in the rock dust with the soil (i.e. simulating ploughing), by introducing the two pool ANC model that was based on an agitated soil-RD suspension study, and by estimating the *in situ* soil pH for the models using an IS-EC calibration. Of course further weathering after these initial years in the field will depend on changes in soil solution chemistry around the rock particles which will in turn be driven by mass transport processes, incomplete wetted surfaces and secondary precipitates all are strongly influenced by climate, soil-biota and acidifying inputs (Vicca et al., 2022; White and Brantley, 2003). Therefore, mass-balance studies that include precipitation monitoring and leachate composition are needed when studying weathering rates on the longer-term scale (Hildebrand and Schack-Kirchner, 2000). However, the studies attempting to make these mass-balances in the lab, e.g. for carbon capture purposes, often use larger doses (>50 Mg/ha) with study limitations such as too short study duration resulting in most of the leaching and pH variability being explained by RD's fast ANC-fractions and not by the slow ANC-fractions (te Pas et al., 2023). The slow ANC-fraction is nevertheless the most relevant pool that will determine the weathering for the years to come. It is thus proposed to focus further studies of RD dissolution in soils after both initial screening with agitated soil-RD suspensions of these ANC-fractions or performing the experiments including treatments of RD where the fast ANC-fractions have been (manually) removed.

5. Conclusion

The objectives of this study were threefold: (1) to compare the dissolution rates between RDs depending on their mineralogy and specific surface area, (2) to study dissolution of RD in soils varying in initial pH and pH buffer power, and (3) to evaluate appropriate accelerated weathering tests to predict the efficiency of rock dust (RD) amendments in restoring soil pH. Four experiments were evaluated that varied in duration and complexity, including batch renewal accelerated weathering, pH_{stat} titration, agitated soil-RD suspension, and mesocosm setups.

Our first hypothesis was confirmed that RD weathering rates largely depend on their mineralogy and SSA_{BET} as the measured rates in pH_{stat} titration coincided quite well to weighted-average mineral dissolution

rates found in literature. The pH-dependent slope of dissolution rates varied substantially depending on the dominant dissolving minerals, which opens opportunities to either limit the risk of overdosing (higher slope) or to have faster dissolution at elevated pH (lower slope) depending on the desired target pH of the soil.

The second hypothesis, was evidenced by proving that, on the one hand, the opportunity of RDs on more acidified soils, which drives RD dissolution leading to higher RD ANCs, and, on the other hand, the associated higher soil pH increase for soils with a lower pH buffer power, e.g. soils with a lower clay and SOM content. Due to the low starting pH of acid sandy forest soils, most RDs applied at a rate of 12 Mg/ha depleted slow ANC-fractions already after one year. Hence, higher doses (25–50 Mg/ha) are needed to raise soil pH above pH 5 which inevitably leads to a substantial cost of application. Therefore and depending on the context of the application, we suggest mixing lime (e.g. 3–5 Mg/ha) with RD (e.g. 15–25 Mg/ha) as a potential solution to sufficiently raise soil pH at an acceptable cost while still having sustainable slow-release buffering by the RD. That is when selecting a RD with a low slope n (e.g. minerals such as biotite, nepheline, hornblende) that still effectively dissolve above pH 5.

Third, a pH-dependent weathering model was developed using rate constants from pH_{stat} tests and three ANC-estimates that were obtained via the three laboratory experiments. The model enabled remarkable accurate prediction of mesocosm soil pH evolution over a period of approximately two years, and including ANC-estimates from soil-RD suspension tests improved -as hypothesized- both accuracy and precision of the prediction. The consumed ANC after two years ranged from 500 to 5000 $mmol_c$/kg RD (2.5–25 % of that of $CaCO_3$), with again the size of the ANC being largely influenced by RD mineralogy and its specific surface area but also by the soil context, and in casu the initial pH and pH buffer power. In conclusion, the variability in RD ANCs and dissolution rates is substantial but the selection of an appropriate RD and dose for soil pH restoration can be confidently made in the laboratory with the presented pH_{stat} and soil-RD suspension methodology.

Author contributions

RV and ES designed the study, RV collected the data, RV and ES analysed the data, RV compiled the manuscript, and all authors contributed to the interpretation of the data and the final manuscript.

CRediT authorship contribution statement

Robrecht Van Der Bauwhede: Conceptualization, Data curation, Formal analysis, Funding acquisition, Investigation, Methodology, Project administration, Resources, Software, Validation, Visualization, Writing – original draft, Writing – review & editing. **Bart Muys:** Conceptualization, Funding acquisition, Investigation, Project administration, Resources, Supervision, Writing – original draft, Writing – review & editing. **Karen Vancampenhout:** Conceptualization, Funding acquisition, Investigation, Methodology, Project administration, Resources, Writing – review & editing. **Erik Smolders:** Conceptualization, Data curation, Formal analysis, Funding acquisition, Investigation, Methodology, Project administration, Resources, Software, Validation, Writing – review & editing.

Declaration of competing interest

The authors declare that they have no known competing financial interests or personal relationships that could have appeared to influence the work reported in this paper.

Data availability

Data will be made available on request.

Acknowledgements

We would like to thank Dries Grauwels, Karla Moors, Kristin Coorevits, Jordi Troonbeeckx, and Iris Serbest for their contribution to the batch titration experiment. Elvira Vassilieva is thanked for her support with the digestion of the RDs. Nancy Weyns is recognized for the mineralogical characterization via XRD-analysis. Lore Fondu is thanked for the assistance in the determination of particle size distribution. Next, the ICP-MS and ICP-OES team are thanked for the analyses of the extracts. Furthermore, Haana Hubrechts, Mara Vervecken, Lennert Aerts, Ides Peeters, Jordi Troonbeeckx, Nele Schillebeeks, and Iris Serbest had a valuable contribution to the execution of the mesocosm experiment. Dr. Toon van Dael is warmly acknowledged for the proof-reading of the first manuscript. We thank the three anonymous reviewers for their in-depth comments that in our opinion greatly improved the manuscript. Financially, we thank Agentschap voor Natuur en Bos, Bosgroep Zuid Nederland, and more specifically for their assistance Dr. Leon van den Berg (Bosgroep), ir. Wim Buysse (ANB) and Mario De Block (ANB) are thanked for the selection of relevant soils. We also thank KU Leuven IOF C3 funding (C3/22/005) and ANB funding (ANB-AB-2023-181) for the supplied resources. R.V. holds a SB-doctoral fellowship of the Research Foundation Flanders (FWO-SB 1S29021N) during the execution of these experiments.

Appendix A. Supplementary data

Supplementary data to this article can be found online at https://doi.org/10.1016/j.geoderma.2023.116734.

References

Aitken, R.L., Moody, P.W., Mckinley, P.G., 1990. Lime requirement of acidic Queensland soils. I. Relationships between soil properties and pH buffer capacity. Soil Res. 28, 695–701. https://doi.org/10.1071/sr9900695.

Amrhein, C., Suarez, D.L., 1988. The use of a surface complexation model to describe the kinetics of ligand-promoted dissolution of anorthite. Geochim. Cosmochim. Acta 52, 2785–2793. https://doi.org/10.1016/0016-7037(88)90146-9.

Anderson, S.P., Dietrich, W.E., Brimhall Jr., G.H., 2002. Weathering profiles, mass-balance analysis, and rates of solute loss: Linkages between weathering and erosion in a small, steep catchment. GSA Bull. 114, 1143–1158. https://doi.org/10.1130/0016-7606(2002)114<1143:WPMBAA>2.0.CO;2.

Barral Silva, M.T., Silva Hermo, B., García-Rodeja, E., Vázquez Freire, N., 2005. Reutilization of granite powder as an amendment and fertilizer for acid soils. Chemosphere 61, 993–1002. https://doi.org/10.1016/j.chemosphere.2005.03.010.

Basak, B.B., Sarkar, B., Maity, A., Chari, M.S., Banerjee, A., Biswas, D.R., 2023. Low-grade silicate minerals as value-added natural potash fertilizer in deeply weathered tropical soil. Geoderma 433, 116433. https://doi.org/10.1016/j.geoderma.2023.116433.

Bates, D., Mächler, M., Bolker, B., Walker, S., 2014. Fitting Linear Mixed-Effects Models using lme4. doi: 10.48550/arXiv.1406.5823.

Bates, D.M., Watts, D.G., 1988. Nonlinear regression analysis and its applications. Wiley.

Bauhus, J., Vor, T., Bartsch, N., Cowling, A., 2004. The effects of gaps and liming on forest floor decomposition and soil C and N dynamics in a Fagus sylvatica forest. Can. J. for. Res. 34, 509–518. https://doi.org/10.1139/x03-218.

Beerling, D.J., Leake, J.R., Long, S.P., Scholes, J.D., Ton, J., Nelson, P.N., Bird, M., Kantzas, E., Taylor, L.L., Sarkar, B., Kelland, M., DeLucia, E., Kantola, I., Müller, C., Rau, G., Hansen, J., 2018. Farming with crops and rocks to address global climate, food and soil security. Nat. Plants 4, 138–147. https://doi.org/10.1038/s41477-018-0108-y.

Beerten, K., Vandersmissen, N., Deforce, K., Vandenberghe, N., 2014. Late Quaternary (15 ka to present) development of a sandy landscape in the Mol area, Campine region, north-east Belgium. J. Quat. Sci. 29, 433–444. https://doi.org/10.1002/jqs.2713.

Blum, A., Lasaga, A., 1988. Role of surface speciation in the low-temperature dissolution of minerals. Nature 331, 431–433. https://doi.org/10.1038/331431a0.

Bobbink, R., Ashmore, M., Braun, S., Flückiger, W., Wyngaert, I.J.J., 2023. Empirical nitrogen critical loads for natural and semi-natural ecosystems: 2002 update.

Bockheim, J.G., Gennadiyev, A.N., Hartemink, A.E., Brevik, E.C., 2014. Soil-forming factors and Soil Taxonomy. Geoderma 226–227, 231–237. https://doi.org/10.1016/j.geoderma.2014.02.016.

Bowen, N.L., 1922. The Reaction Principle in Petrogenesis. J. Geol. 30, 177–198. https://doi.org/10.1086/622871.

Brahy, V., Deckers, J., Delvaux, B., 2000. Estimation of soil weathering stage and acid neutralizing capacity in a toposequence Luvisol-Cambisol on loess under deciduous forest in Belgium. Eur. J. Soil Sci. 51, 1–13. https://doi.org/10.1046/j.1365-2389.2000.00285.x.

Brantley, S.L., Lebedeva, M., 2011. Learning to Read the Chemistry of Regolith to Understand the Critical Zone. Annu. Rev. Earth Planet. Sci. 39, 387–416. https://doi.org/10.1146/annurev-earth-040809-152321.

Brazil, 2016. Instrução Normativa Nº 05 de 10 de março de 2016 532 [WWW Document]. URL https://www.gov.br/agricultura/pt-br/assuntos/insumos-agropecuarios/insumos-agricolas/fertilizantes/legislacao/in-5-de-10-3-16-remineralizadores-e-substratos-para-plantas.pdf.

Brunauer, S., Emmett, P.H., Teller, E., 1938. Adsorption of Gases in Multimolecular Layers. J. Am. Chem. Soc. 60, 309–319. https://doi.org/10.1021/ja01269a023.

Burke, M.K., Raynal, D.J., 1998. Liming influences growth and nutrient balances in sugar maple (Acer saccharum) seedlings on an acidic forest soil. Environ. Exp. Bot. 39, 105–116. https://doi.org/10.1016/S0098-8472(97)00029-4.

Calabrese, S., Wild, B., Bertagni, M.B., Bourg, I.C., White, C., Aburto, F., Cipolla, G., Noto, L.V., Porporato, A., 2022. Nano- to Global-Scale Uncertainties in Terrestrial Enhanced Weathering. Environ. Sci. Technol. 56, 15261–15272. https://doi.org/10.1021/acs.est.2c03163.

Cappuyns, V., Swennen, R., 2008. The application of pHstat leaching tests to assess the pH-dependent release of trace metals from soils, sediments and waste materials. J. Hazard. Mater. 158, 185–195. https://doi.org/10.1016/j.jhazmat.2008.01.058.

Casey, W.H., Sposito, G., 1992. On the temperature dependence of mineral dissolution rates. Geochim. Cosmochim. Acta 56, 3825–3830. https://doi.org/10.1016/0016-7037(92)90173-G.

Chadwick, O.A., Chorover, J., 2001. The chemistry of pedogenic thresholds. Geoderma, Developments and Trends in Soil Science 100, 321–353. https://doi.org/10.1016/S0016-7061(01)00027-1.

Ciesielski, O.A., Sterckeman, T., 1997. Determination of cation exchange capacity and exchangeable cations in soils by means of cobalt hexamine trichloride. Effects of experimental conditions. Agronomie 17, 1–7.

Court, M., van der Heijden, G., Didier, S., Nys, C., Richter, C., Pousse, N., Saint-André, L., Legout, A., 2018. Long-term effects of forest liming on mineral soil, organic layer and foliage chemistry: Insights from multiple beech experimental sites in Northern France. For. Ecol. Manag. 409, 872–889. https://doi.org/10.1016/j.foreco.2017.12.007.

Curtin, D., Smillie, G.W., 1983. Soil Solution Composition as Affected by Liming and Incubation. Soil Sci. Soc. Am. J. 47, 701–707. https://doi.org/10.2136/sssaj1983.03615995004700040020x.

Daval, D., Calvaruso, C., Guyot, F., Turpault, M.-P., 2018. Time-dependent feldspar dissolution rates resulting from surface passivation: Experimental evidence and geochemical implications. Earth Planet. Sci. Lett. 498, 226–236. https://doi.org/10.1016/j.epsl.2018.06.035.

de Vries, W., de Jong, A., Kros, J., Spijker, J., 2021. The use of soil nutrient balances in deriving forest biomass harvesting guidelines specific to region, tree species and soil type in the Netherlands. For. Ecol. Manag. 479, 118591 https://doi.org/10.1016/j.foreco.2020.118591.

FAO, SER, IUCN/CEM, 2023. Standards of practice to guide ecosystem restoration: A contribution to the United Nations Decade on Ecosystem Restoration: Summary report. FAO, Rome, Italy. doi: 10.4060/cc5223en.

García-Gómez, H., Garrido, J.L., Vivanco, M.G., Lassaletta, L., Rábago, I., Àvila, A., Tsyro, S., Sánchez, G., González Ortiz, A., González-Fernández, I., Alonso, R., 2014. Nitrogen deposition in Spain: Modeled patterns and threatened habitats within the Natura 2000 network. Sci. Total Environ. 485–486, 450–460. https://doi.org/10.1016/j.scitotenv.2014.03.112.

Garnier, S., Ross, N., Rudis, B., Sciaini, M., Camargo, A.P., Scherer, C., 2021. viridis: Colorblind-Friendly Color Maps for R.

Gillman, G.P., Burkett, D.C., Coventry, R.J., 2002. Amending highly weathered soils with finely ground basalt rock. Appl. Geochem. 17, 987–1001. https://doi.org/10.1016/S0883-2927(02)00078-1.

Graveland, J., van der Wal, R., van Balen, J.H., van Noordwijk, A.J., 1994. Poor reproduction in forest passerines from decline of snail abundance on acidified soils. Nature 368, 446–448. https://doi.org/10.1038/368446a0.

Gruber, C., Zhu, C., Georg, R.B., Zakon, Y., Ganor, J., 2014. Resolving the gap between laboratory and field rates of feldspar weathering. Geochim. Cosmochim. Acta 147, 90–106. https://doi.org/10.1016/j.gca.2014.10.013.

Gudbrandsson, S., Wolff-Boenisch, D., Gislason, S.R., Oelkers, E.H., 2011. An experimental study of crystalline basalt dissolution from 2≤pH≤11 and temperatures from 5 to 75°C. Geochim. Cosmochim. Acta 75, 5496–5509. https://doi.org/10.1016/j.gca.2011.06.035.

Gudbrandsson, S., Wolff-Boenisch, D., Gislason, S.R., Oelkers, E.H., 2014. Experimental determination of plagioclase dissolution rates as a function of its composition and pH at 22°C. Geochim. Cosmochim. Acta 139, 154–172. https://doi.org/10.1016/j.gca.2014.04.028.

Guidelines for soil description, 4th ed. ed, 2006. . Food and Agriculture Organization of the United Nations, Rome.

Hamilton, J.P., Brantley, S.L., Pantano, C.G., Criscenti, L.J., Kubicki, J.D., 2001. Dissolution of nepheline, jadeite and albite glasses: toward better models for aluminosilicate dissolution. Geochim. Cosmochim. Acta 65, 3683–3702. https://doi.org/10.1016/S0016-7037(01)00724-4.

Heřmanská, M., Voigt, M.J., Marieni, C., Declercq, J., Oelkers, E.H., 2022. A comprehensive and internally consistent mineral dissolution rate database: Part I: Primary silicate minerals and glasses. Chem. Geol. 597, 120807 https://doi.org/10.1016/j.chemgeo.2022.120807.

Hildebrand, E.E., Schack-Kirchner, H., 2000. Initial effects of lime and rock powder application on soil solution chemistry in a dystric cambisol – results of model experiments. Nutr. Cycl. Agroecosystems 56, 69–78. https://doi.org/10.1023/A:1009714927385.

Hoettl, R.F., Zoettl, H.W., 1993. Liming as a mitigation tool in Germany's declining forests reviewing results from former and recent trials. For. Ecol. Manag. 325–338 https://doi.org/10.1016/0378-1127(93)90209-6.

Jacobsen, B.H., Latacz-Lohmann, U., Luesink, H., Michels, R., Ståhl, L., 2019. Costs of regulating ammonia emissions from livestock farms near Natura 2000 areas - analyses of case farms from Germany, Netherlands and Denmark. J. Environ. Manage. 246, 897–908. https://doi.org/10.1016/j.jenvman.2019.05.106.

Jansone, L., von Wilpert, K., Hartmann, P., 2020. Natural Recovery and Liming Effects in Acidified Forest Soils in SW-Germany. Soil Syst. 4, 38. https://doi.org/10.3390/soilsystems4030038.

Kalinowski, B.E., Schweda, P., 1996. Kinetics of muscovite, phlogopite, and biotite dissolution and alteration at pH 1–4, room temperature. Geochim. Cosmochim. Acta 60, 367–385. https://doi.org/10.1016/0016-7037(95)00411-4.

Kantola, I.B., Blanc-Betes, E., Masters, M.D., Chang, E., Marklein, A., Moore, C.E., von Haden, A., Bernacchi, C.J., Wolf, A., Epihov, D.Z., Beerling, D.J., DeLucia, E.H., 2023. Improved net carbon budgets in the US Midwest through direct measured impacts of enhanced weathering. Glob. Change Biol. Online Version of Record before inclusion in an issue. doi: 10.1111/gcb.16903.

Kelland, M.E., Wade, P.W., Lewis, A.L., Taylor, L.L., Sarkar, B., Andrews, M.G., Lomas, M.R., Cotton, T.E.A., Kemp, S.J., James, R.H., Pearce, C.R., Hartley, S.E., Hodson, M.E., Leake, J.R., Banwart, S.A., Beerling, D.J., 2020. Increased yield and CO2 sequestration potential with the C4 cereal Sorghum bicolor cultivated in basaltic rock dust-amended agricultural soil. Glob. Change Biol. 26, 3658–3676. https://doi.org/10.1111/gcb.15089.

Kjøller, R., Clemmensen, K.E., 2009. Belowground ectomycorrhizal fungal communities respond to liming in three southern Swedish coniferous forest stands. For. Ecol. Manag. 257, 2217–2225. https://doi.org/10.1016/j.foreco.2009.02.038.

Knauss, K.G., Nguyen, S.N., Weed, H.C., 1993. Diopside dissolution kinetics as a function of pH, CO2, temperature, and time. Geochim. Cosmochim. Acta 57, 285–294. https://doi.org/10.1016/0016-7037(93)90431-U.

Kohler, M., Kunz, J., Herrmann, J., Hartmann, P., Jansone, L., Puhlmann, H., von Wilpert, K., Bauhus, J., 2019. The Potential of Liming to Improve Drought Tolerance of Norway Spruce [Picea abies (L.) Karst.]. Front. Plant Sci. 10.

Kronberg, B.I., Nesbitt, H.W., 1981. Quantification of Weathering, Soil Geochemistry and Soil Fertility. J. Soil Sci. 32, 453–459. https://doi.org/10.1111/j.1365-2389.1981.tb01721.x.

Langmuir, D., 1997. Aqueous Environmental Geochemistry. Prentice-Hall Inc, Upper Saddle River, New Jersey.

Lasaga, A.C., Soler, J.M., Ganor, J., Burch, T.E., Nagy, K.L., 1994. Chemical weathering rate laws and global geochemical cycles. Geochim. Cosmochim. Acta 58, 2361–2386. https://doi.org/10.1016/0016-7037(94)90016-7.

Lenth, R.V., 2016. Least-Squares Means: The R Package lsmeans. J. Stat. Softw. 69, 1–33. https://doi.org/10.18637/jss.v069.i01.

Lewis, A.L., Sarkar, B., Wade, P., Kemp, S.J., Hodson, M.E., Taylor, L.L., Yeong, K.L., Davies, K., Nelson, P.N., Bird, M.I., Kantola, I.B., Masters, M.D., DeLucia, E., Leake, J.R., Banwart, S.A., Beerling, D.J., 2021. Effects of mineralogy, chemistry and physical properties of basalts on carbon capture potential and plant-nutrient element release via enhanced weathering. Appl. Geochem. 132, 105023 https://doi.org/10.1016/j.apgeochem.2021.105023.

Li, L., Maher, K., Navarre-Sitchler, A., Druhan, J., Meile, C., Lawrence, C., Moore, J., Perdrial, J., Sullivan, P., Thompson, A., Jin, L., Bolton, E.W., Brantley, S.L., Dietrich, W.E., Mayer, K.U., Steefel, C.I., Valocchi, A., Zachara, J., Kocar, B., Mcintosh, J., Tutolo, B.M., Kumar, M., Sonnenthal, E., Bao, C., Beisman, J., 2017. Expanding the role of reactive transport models in critical zone processes. Earth-Sci. Rev. 165, 280–301. https://doi.org/10.1016/j.earscirev.2016.09.001.

Manning, D.A.C., Theodoro, S.H., 2020. Enabling food security through use of local rocks and minerals. Extr. Ind. Soc. 7, 480–487. https://doi.org/10.1016/j.exis.2018.11.002.

Marschner, B., Waldemar Wilczynski, A., 1991. The effect of liming on quantity and chemical composition of soil organic matter in a pine forest in Berlin, Germany. Plant Soil 137, 229–236. https://doi.org/10.1007/BF00011201.

McMillan, W.G., Teller, E., 2002. The Assumptions of the B.E.T. Theory. [WWW Document]. ACS Publ. doi: 10.1021/j150484a003.

Moore, J.-D., Ouimet, R., 2021. Liming still positively influences sugar maple nutrition, vigor and growth, 20 years after a single application. For. Ecol. Manag. 490, 119103 https://doi.org/10.1016/j.foreco.2021.119103.

Muys, B., Beckers, G., Nachtergale, L., Lust, N., Merckx, R., Granval, P., 2003. Medium-term evaluation of a forest soil restoration trial combining tree species change, fertilisation and earthworm introduction: The 7th international symposium on earthworm ecology · Cardiff · Wales · 2002. Pedobiologia 47, 772–783. https://doi.org/10.1078/0031-4056-00257.

Nilsson, J., 1988. Critical Loads for Sulphur and Nitrogen. In: Mathy, P. (Ed.), Air Pollution and Ecosystems. Springer, Netherlands, Dordrecht, pp. 85–91. https://doi.org/10.1007/978-94-009-4003-1_11.

Oates, J.A.H., 2008. Lime and Limestone: Chemistry and Technology, Production and Uses. John Wiley & Sons.

Oelkers, E.H., Schott, J., Devidal, J.-L., 1994. The effect of aluminum, pH, and chemical affinity on the rates of aluminosilicate dissolution reactions. Geochim. Cosmochim. Acta 58, 2011–2024. https://doi.org/10.1016/0016-7037(94)90281-X.

Ramos, C.G., Querol, X., Oliveira, M.L.S., Pires, K., Kautzmann, R.M., Oliveira, L.F.S., 2015. A preliminary evaluation of volcanic rock powder for application in agriculture as soil a remineralizer. Sci. Total Environ. 512–513, 371–380. https://doi.org/10.1016/j.scitotenv.2014.12.070.

Ramos, C.G., Hower, J.C., Blanco, E., Oliveira, M.L.S., Theodoro, S.H., 2022. Possibilities of using silicate rock powder: An overview. Geosci. Front. 13, 101185 https://doi.org/10.1016/j.gsf.2021.101185.

Rdc, T., 2009. a language and environment for statistical computing. HttpwwwR-Proj.
Rinder, T., von Hagke, C., 2021. The influence of particle size on the potential of enhanced basalt weathering for carbon dioxide removal - Insights from a regional assessment. J. Clean. Prod. 315, 128178 https://doi.org/10.1016/j.jclepro.2021.128178.
Robertson, G.P., 1999. Standard Soil Methods for Long-term Ecological Research. Oxford University Press.
Schofield, R.K., Taylor, A.W., 1955. The Measurement of Soil pH. Soil Sci. Soc. Am. J. 19, 164–167. https://doi.org/10.2136/sssaj1955.03615995001900020013x.
Schulte-Uebbing, L.F., Beusen, A.H.W., Bouwman, A.F., de Vries, W., 2022. From planetary to regional boundaries for agricultural nitrogen pollution. Nature 610, 507–512. https://doi.org/10.1038/s41586-022-05158-2.
Schulze, E.-. D., De Vries, W., Hauhs, M., Rosén, K., Rasmussen, L., Tamm, C.-O., Nilsson, J., 1989. Critical loads for nitrogen deposition on forest ecosystems. Water. Air. Soil Pollut. 48, 451–456. doi: 10.1007/BF00283342.
Schwarz, A., Wilcke, W., Zech, W., Stýk, J., 1999. Heavy Metal Release from Soils in Batch pHstat Experiments. Soil Sci. Soc. Am. J. 63, 290–296. https://doi.org/10.2136/sssaj1999.03615995006300020006x.
Siepel, H., Bobbink, R., van de Riet, B.P., van den Burg, A.B., Jongejans, E., 2019. Long-term effects of liming on soil physico-chemical properties and micro-arthropod communities in Scotch pine forest. Biol. Fertil. Soils 55, 675–683. https://doi.org/10.1007/s00374-019-01378-3.
Slessarev, E.W., Lin, Y., Bingham, N.L., Johnson, J.E., Dai, Y., Schimel, J.P., Chadwick, O. A., 2016. Water balance creates a threshold in soil pH at the global scale. Nature 540, 567–569. https://doi.org/10.1038/nature20139.
Strefler, J., Amann, T., Bauer, N., Kriegler, E., Hartmann, J., 2018. Potential and costs of carbon dioxide removal by enhanced weathering of rocks. Environ. Res. Lett. 13, 034010 https://doi.org/10.1088/1748-9326/aaa9c4.
Sverdrup, H., Warfvinge, P., 1993. Calculating field weathering rates using a mechanistic geochemical model PROFILE. Appl. Geochem. 8, 273–283. https://doi.org/10.1016/0883-2927(93)90042-F.
Swoboda, P., Döring, T.F., Hamer, M., 2022. Remineralizing soils? The agricultural usage of silicate rock powders: A review. Sci. Total Environ. 807, 150976 https://doi.org/10.1016/j.scitotenv.2021.150976.
Taylor, L.L., Driscoll, C.T., Groffman, P.M., Rau, G.H., Blum, J.D., Beerling, D.J., 2021. Increased carbon capture by a silicate-treated forested watershed affected by acid deposition. Biogeosciences 18, 169–188. https://doi.org/10.5194/bg-18-169-2021.
te Pas, E.E.E.M. te, Hagens, M., Comans, R.N.J., 2023. Assessment of the enhanced weathering potential of different silicate minerals to improve soil quality and sequester CO_2. Front. Clim. 4. doi: 10.3389/fclim.2022.954064.
Ulrich, B., Sumner, M.E., 2012. Soil Acidity. Springer Science & Business Media.
van Diggelen, R., Bergsma, H., Bobbink, R., Sevink, J., Siebel, H., Siepel, H., Vogels, J., de Vries, W., 2019. Steenmeel en natuurherstel: een gelukkige relatie of een risicovolle combinatie?.
van Straaten, P., 2006. Farming with rocks and minerals: challenges and opportunities. An. Acad. Bras. Ciênc. 78, 731–747. https://doi.org/10.1590/S0001-37652006000400009.
Velbel, M.A., 1993. Constancy of silicate-mineral weathering-rate ratios between natural and experimental weathering: implications for hydrologic control of differences in absolute rates. Chem. Geol., Geochemical kinetics of mineral-water reactions in the field and the laboratory 105, 89–99. doi: 10.1016/0009-2541(93)90120-8.
Vicca, S., Goll, D.S., Hagens, M., Hartmann, J., Janssens, I.A., Neubeck, A., Peñuelas, J., Poblador, S., Rijnders, J., Sardans, J., Struyf, E., Swoboda, P., van Groenigen, J.W., Vienne, A., Verbruggen, E., 2022. Is the climate change mitigation effect of enhanced silicate weathering governed by biological processes? Glob. Change Biol. 28, 711–726. https://doi.org/10.1111/gcb.15993.
Vienne, A., Poblador, S., Portillo-Estrada, M., Hartmann, J., Ijiehon, S., Wade, P., Vicca, S., 2022. Enhanced Weathering Using Basalt Rock Powder: Carbon Sequestration, Co-benefits and Risks in a Mesocosm Study With Solanum tuberosum. Front. Clim. 4.
Vitousek, P., Chadwick, O., 2013. Pedogenic Thresholds and Soil Process Domains in Basalt-Derived Soils. Ecosystems 16. https://doi.org/10.1007/s10021-013-9690-z.
Vogels, J.J., Van de Waal, D.B., WallisDeVries, M.F., Van den Burg, A.B., Nijssen, M., Bobbink, R., Berg, M.P., Olde Venterink, H., Siepel, H., 2023. Towards a mechanistic understanding of the impacts of nitrogen deposition on producer–consumer interactions. Biol. Rev. 98, 1712–1731. https://doi.org/10.1111/brv.12972.
Wakatsuki, T., Rasyidin, A., 1992. Rates of weathering and soil formation. Geoderma 52, 251–263. https://doi.org/10.1016/0016-7061(92)90040-E.
Walker, W.J., Cronan, C.S., Patterson, H.H., 1988. A kinetic study of aluminum adsorption by aluminosilicate clay minerals. Geochim. Cosmochim. Acta 52, 55–62. https://doi.org/10.1016/0016-7037(88)90056-7.
West, T.O., McBride, A.C., 2005. The contribution of agricultural lime to carbon dioxide emissions in the United States: dissolution, transport, and net emissions. Agric. Ecosyst. Environ. 108, 145–154. https://doi.org/10.1016/j.agee.2005.01.002.
White, A.F., Brantley, S.L., 2003. The effect of time on the weathering of silicate minerals: why do weathering rates differ in the laboratory and field? Chem. Geol. Controls on Chemical Weathering 202, 479–506. https://doi.org/10.1016/j.chemgeo.2003.03.001.
Wickham, H., 2011. ggplot2. Wires Comput. Stat. 3, 180–185. https://doi.org/10.1002/wics.147.
Zhang, H., Bloom, P.R., Nater, E.A., Susan Erich, M., 1996. Rates and stoichiometry of hornblende dissolution over 115 days of laboratory weathering at pH 3.6–4.0 and 25 °C in 0.01 M lithium acetate. Geochim. Cosmochim. Acta 60, 941–950. https://doi.org/10.1016/0016-7037(95)00447-5.